Phase relations of Fe-Ni alloys at high pressure and temperature

Wendy L. Mao[a,e,f,*], Andrew J. Campbell[a,b,g], Dion L. Heinz[a,c], and Guoyin Shen[d,h]

[a]Department of the Geophysical Sciences, [b]Chicago Center for Cosmochemistry, [c]James Franck Institute, and [d]Consortium for Advanced Radiation Sources, The University of Chicago, Chicago, IL 60637 USA, [e]Geophysical Laboratory, Carnegie Institution of Washington, Washington, D.C. 20015 USA, [f]Present address: Lujan Neutron Scattering Center, Los Alamos National Laboratory, Los Alamos, NM 87545 USA, [g]Present address: Department of Geology, University of Maryland, College Park, MD 20742 USA, [h]Present address: HPCAT, Advanced Photon Source, Argonne National Laboratory, Argonne, IL 60439

Abstract

Using a diamond anvil cell and double-sided laser-heating coupled with synchrotron x-ray diffraction, we determined phase relations for three compositions of Fe-rich FeNi alloys *in situ* at high pressure and high temperature. We studied Fe with 5 wt%, 15 wt%, and 20 wt% Ni to 55 GPa, 62 GPa, and 72 GPa respectively at temperatures up to ~3000 K. Ni stabilizes the face centered cubic phase to lower temperatures and higher pressure, and this effect increases with increasing pressure. Extrapolation of our experimental results for Fe with 15 wt% Ni suggests that the stable phase at inner core conditions is hexagonal close packed, although if the temperature at the inner core boundary is higher than ~6400 K, a two phase outer region may also exist. Comparison to previous laser-heated diamond anvil cell studies demonstrates the importance of kinetics even at high temperatures.

Keywords: Iron-Nickel alloys; Earth's core; High pressure; Diamond anvil cell; Laser-heating; X-ray Diffraction

*corresponding author; Fax: 505-665-2676; *E-mail address*: wmao@lanl.gov

1. Introduction

As major constituents of the Earth's core, Fe and its alloys have long been of great interest to geophysicists (Birch, 1952). From geophysical, cosmochemical, and geodynamic data, it is generally accepted that the core is composed of an Fe-rich Fe-Ni alloy with a small amount of light element(s) (McDonough, 2003; Stixrude and Brown, 1998). Information on the behavior of Fe-Ni alloys at high pressure-temperature (*P*-*T*), such as phase relations and thermal equations of state (EOS), is essential for interpreting seismic and geomagnetic observations and for numerical modeling of the Earth's deep interior.

While pure Fe at high *P*-*T* has been the subject of numerous studies, there are far fewer studies on Fe-Ni alloys. At ambient conditions, the stable phase of Fe is the body-centered cubic (bcc) structure. This phase, α-Fe, transforms into a face-centered cubic (fcc or γ-Fe) phase upon increasing temperature above 1185 K, and then transforms to another bcc (δ-Fe) phase before melting (Hemley and Mao, 2001). At high pressure, both bcc and fcc Fe transform into the hexagonal close-packed (hcp or ε) phase (Takahashi and Bassett, 1964). This phase has a broad stability region, and Fe is generally considered to be stable in the hcp structure at inner core conditions (Hemley and Mao, 2001; Ma et al., 2004).

Previous work on the quasihydrostatic compression of $Fe_{0.8}Ni_{0.2}$ (Mao et al., 1990) are the only results to core pressures, but they were measured at ambient temperature. At high pressure Ni has been shown to stabilize the face-centered cubic (fcc) phase (Huang et al., 1988; Lin et al., 2002). Externally heated diamond anvil cell (DAC) studies on a number of Fe-Ni alloys with up to 35 wt% Ni indicate that the core may consist of both a fcc and hcp phase (Huang et al., 1988; Huang et al., 1992), but these studies require

significant extrapolation for application to the core. Recent laser-heated DAC (LHDAC) results on Fe with 10 wt% Ni were conducted to much higher temperatures and suggest that the inner core should be in the hcp structure (Lin, 2002). It is necessary to further explore the compositional effect of Ni on the *P-T-x* phase diagram of Fe-Ni alloys at high *P-T* and relevant core compositions to determine the effect on core properties. This would serve as a baseline for understanding the additional effects of the presence of potential light elements in the core.

2. Experimental

Three compositions of Fe-rich Fe-Ni alloys were investigated. Fe15%Ni and Fe20%Ni refer to synthetic alloys of Fe with 15 wt% (14.4 mol%) Ni and 20 wt% (19.2 mol%) Ni respectively. In this paper Fe5%Ni refers to filings from a natural sample of the Negrillos (IIAB) iron meteorite which contains 5.4 wt% (5.2 mol%) Ni. This specimen also contains minor amounts of other elements, most notably Co (0.4 wt%) and P (0.1-0.2 wt%). This composition is probably similar to the Earth's core minus the light element component (McDonough, 2003). Small foils of sample (7 μm thick, 50 μm diameter) were sandwiched between thin (7 μm) layers of NaCl which acted as a thermal insulator, pressure-transmitting medium, and internal pressure standard (Heinz and Jeanloz, 1994; Sata et al., 2002). The pressure was calculated from the ambient temperature NaCl EOS before heating, similar to the previous Fe-Ni alloy LHDAC study (Lin et al., 2003). The sample assemblage was loaded into a ~100 μm diameter chamber that was drilled into a pre-indented stainless steel gasket in a symmetric DAC.

Monochromatic synchrotron x-radiation (λ = 0.3344 Å) at GSECARS 13-IDD beamline of the Advanced Photon Source (APS), Argonne National Laboratory (ANL) was used for angle-dispersive x-ray diffraction measurements. The x-ray beam was focused in the horizontal and vertical direction to a 5 x 7 μm (FWHM) spot using Kirkpatrick-Baez mirrors. Diffraction patterns were taken using a Bruker CCD detector *in situ* at high *P-T*. A CeO_2 standard was used to calibrate the sample to detector distance and the detector tilt. An x-ray transparent cubic boron nitride seat was used to support the downstream diamond in order to increase 2θ access from the sample down to d-spacings of 0.8 Å.

A double-sided Nd:YLF laser system operating in the Gaussian TEM_{00} mode was used to heat the sample (Shen et al., 2001). Temperature was determined using spectral radiometry by fitting the thermal radiation spectrum to the Planck radiation function. Temperature measurements taken by the spectral radiometry system at 13-IDD have been verified prior to our experiments. The major source of potential error in temperature is the lack of information regarding the wavelength dependence of emissivity. The wavelength range used for the temperature fit was 670-830 nm which represents a compromise between reducing the error from emissivity by reducing the wavelength range, while also having a large enough range to avoid introduction of errors from some non-linear portion of the system response (Shen et al., 2001). The laser beam diameter was approximately 25 μm, producing a stable heated spot much larger than the focused x-ray beam. Axial and radial temperature gradients were minimized by the use of the NaCl insulating layers. The maximized heating area and minimized temperature gradients help reduce errors associated with chromatic aberration. The temperature uncertainty (1σ) for multiple temperature

68 measurements and the temperature difference measured from both sides of the sample was
69 approximately 100 K.
70
71 **3. Results and Discussion**
72 We investigated the phase boundaries for the hcp + fcc two phase coexistence
73 region by monitoring changes in the x-ray diffraction pattern *in situ* as we laser-heated the
74 sample at high *P*. Each heating cycle was conducted on a new, previously unheated spot to
75 ensure that the composition of the spot probed was the same as the composition of the
76 sample. Upon increasing temperature, we observed the transformation from hcp only to a
77 mixture of hcp + fcc phases to fcc (Figure 1). The hcp → hcp + fcc and hcp + fcc → fcc
78 phase boundaries for varying Ni compositions were determined for the three compositions
79 studied (Figure 2). In the two phase region, the volume difference between the Ni-rich fcc
80 phase and the coexisting Ni-poor hcp phase ($\Delta V^{fcc\text{-}hcp}$) was approximately 1-3% with the
81 difference becoming larger at higher *P-T* (Table 1). This corresponds to an approximate
82 10 wt% difference in Ni content between the fcc and hcp phases (Figure 3). A previous
83 study on Fe10%Ni found a 1% $\Delta V^{fcc\text{-}hcp}$ at 40 GPa and 1602 K (Lin et al., 2002).
84 Reproducibility of results depends on reaching thermodynamic equilibrium. We
85 investigated the importance of kinetics during a number of long heating cycles. For
86 example, it took nearly 30 minutes of laser-heating at ~1400 K to transform the Fe20%Ni
87 sample that was initially a quenched mixture of hcp + fcc phases into hcp only (Figure 5).
88 Even at high temperature, kinetic effects indicate that a significant time may be required
89 for the sample to reach its equilibrium phase assemblage. This may explain why our hcp +
90 fcc coexistence region is narrower than those of the previous laser-heating study (Lin et al.,

2002). Diffusion of Ni appears to be an important issue. Upon decreasing temperature, it was very difficult to completely transform the quenched fcc phase back into the hcp phase. This stubborn nature of the fcc phase has been observed previously in pure Fe and other Fe-rich alloys (Uchida et al., 2001). We mainly determined transition conditions on increasing temperature cycles, but did constrain the phase boundaries on some long heating cycles following a decrease in temperature (Figure 6).

Increasing Ni concentrations stabilize the fcc phase to lower *T* and higher *P*. Even 5 wt% Ni shows significant stabilization of the fcc field relative to pure Fe, and this effect increases with increasing pressure. Figure 3 shows a summary *P-T-x* phase diagram for Fe-rich Fe-Ni compositions. Qualitatively, our results are consistent with previously reported work on different Fe-Ni compositions (Huang et al., 1988; Huang et al., 1992; Lin et al., 2002) and the results for pure Fe (Ma et al., 2004). However, earlier resistively heated DAC studies at higher Ni (up to 35 wt%) concentrations report the hcp + fcc → fcc phase boundary at much lower temperature than would be expected from extrapolation of our data to higher Ni content (Huang et al., 1992). Additional compositions may need to be measured in order to constrain the Fe-Ni phase diagram with higher Ni contents. While a resistively heated DAC provides better temperature control, it is limited to lower temperatures, so the hcp + fcc → fcc boundary has not been reported using this technique for lower Ni concentrations. We observed that the slope of the hcp → hcp + fcc and hcp + fcc → fcc phase boundaries becomes flatter with increasing Ni content which is consistent with previous results, although extrapolation between our 15 wt% Ni data predict a shallower slope than reported for Fe10%Ni (Lin et al., 2002) (Table 2).

Constraining the phase boundary slopes is critical when considering extrapolation of the experimental results to core conditions. The Lindemann law extrapolation of recent LHDAC data gives a melting temperature for pure Fe of 5800 K at the pressure of the inner core boundary (ICB) (Ma et al., 2004). Extrapolation of Fe10%Ni and Fe15%Ni results indicate that hcp would be the stable phase for these compositions for possible core geotherms crossing through 5800 K at ICB pressure (Figure 4). It should be noted that there are many uncertainties in our understanding of the actual ICB temperature. For example, the addition of light elements would depress the melting point and result in a lower ICB temperature (Alfé et al., 2002). However, if our simple linear extrapolation holds, the ICB would have to be ~6400 K for the two phase hcp + fcc to be stable for Fe15%Ni at ICB pressure. If the ICB were at even higher temperature this would stabilize the two phase hcp + fcc region for even lower Ni contents. Then the inner core could comprise an outer two phase hcp + fcc layer and a hcp only innermost core. Whether this has relevance to the observed change in elastic anisotropy in the inner core (Ishii and Dziewonski, 2002) requires further investigation and tighter constraints of the ICB temperature.

Theoretical calculations of pure Fe have resulted in interesting speculations regarding the inner core. Two recent studies suggested that the bcc structure of Fe may be the stable inner core phase (Belonoshko et al., 2003; Vocadlo et al., 2003). It is known from the 1 bar phase diagram that alloying with Ni promotes the fcc phase and supresses the bcc phase in Fe-rich alloys, and as shown in this study, Ni stabilizes the fcc phase even to high *P-T* conditions. We expect that the presence of Ni would counteract the formation of the

hypothesized bcc phase at high *P-T*, but the effect of Ni on the stability of phases should be investigated experimentally to inner core conditions to confirm this.

4. Conclusions

The addition of Ni clearly affects the physics and chemistry of Fe at high *P-T*. In examining phase relations in Fe5%Ni, Fe15%Ni, and Fe25%Ni we found that increasing Ni content stabilizes the fcc phase to lower temperature and higher pressures. Our results are consistent with previous LHDAC studies, but discrepancies with resistively heated DAC studies remain. This may be an issue with kinetics, which was found to be important especially with the fcc phase. Fe-rich Fe-Ni alloys should serve as a baseline composition for comparison to seismic observations and the study of possible light alloying elements. Ni may influence partitioning of minor and trace elements between the solid, inner core and the liquid, outer core. Its effect on the melting curve of Fe also needs to be studied. In general, extension of LHDAC studies to higher *P-T* is needed. In particular, key anchor points for extrapolation of the melting curve and determination the phase(s) in the inner core would be the intersection of the hcp → hcp + fcc boundary and the melting curve and the intersection of the hcp + fcc → fcc boundary and the melting curve.

Acknowledgments

We gratefully acknowledge Dr. Vitali Prakapenka and James Devine for their assistance with the experiments. GSECARS is supported by the National Science Foundation (NSF)-Earth Sciences (EAR) Grant 0217473, Department of Energy (DOE) Geosciences Grant DE-FG02-94ER14466 and the State of Illinois. Use of the APS was supported by the U.S.

158 DOE, Basic Energy Sciences, Office of Energy Research, under Contract No. W-31-109-
159 Eng-38. This work was supported by NSF-EAR Geophysics Grant 0309486.

References

Alfé, D., Gillan, M.J. and Price, G.D., 2002. Composition and temperature of the Earth's core constrained by combining ab initio calculations and seismic data. Earth Planet. Sci. Lett., 195: 91-98.

Belonoshko, A.B., Ahuja, R. and Johansson, B., 2003. Stability of the body-centered-cubic phase of iron in the Earth's inner core. Nature, 424: 1032-1034.

Birch, F., 1952. Elasticity and constitution of the Earth's interior. J. Geophys. Res., 57(2): 227-286.

Heinz, D.L. and Jeanloz, R., 1994. Compression of the B2 high-pressure phase of NaCl. Phys. Rev. B, 30: 6045-6050.

Hemley, R.J. and Mao, H.K., 2001. In-situ studies of iron under pressure: New windows on the Earth's core. Intern. Geol. Rev., 43: 1-30.

Huang, E., Bassett, W.A. and Weathers, M.S., 1988. Phase relationships of Fe-Ni alloys at high pressures and temperatures. J. Geophys. Res., 93: 7741-7746.

Huang, E., Bassett, W.A. and Weathers, M.S., 1992. Phase diagram and elastic properties of Fe 30% Ni alloy by synchrotron. J. Geophys. Res., 97: 4497-4502.

Ishii, M. and Dziewonski, A., 2002. The innermost inner core of the earth: evidence for a change in anisotropic behavior at the radius of about 300 km. Proc. Nat. Aca. Sci., 99: 14026-14030.

Lin, J.-F., 2002. Alloying effects of silicon and nickel on iron in the earth's core, University of Chicago, Chicago, 115 pp.

Lin, J.-F. et al., 2002. Iron-nickel alloy in Earth ’s core? Geophys. Res. Lett., 29(10): doi:10.1029/2002GL015089.

Lin, J.-F. et al., 2003. Sound velocities of iron-nickel and iron-silicon alloys at high pressures. Geophys. Res. Lett., 30(21): doi:10.1029/2003GL018405.

Ma, Y. et al., 2004. In situ X-ray diffraction studies of iron to Earth-core conditions. Phys. Earth Planet. Inter., 143-144: 455-467.

Mao, H.K., Wu, Y., Chen, L.C., Shu, J.F. and Jephcoat, A.P., 1990. Static compression of iron to 300 GPa and $Fe_{0.8}Ni_{0.2}$ alloy to 260 GPa: Implications for composition of the core. J. Geophys. Res., 95: 21,737-21,742.

McDonough, W.F., 2003. Compositional model for the Earth's core. In: R. Carlson (Editor), The Mantle and Core. Elsevier-Pergamon, Oxford, pp. 547-568.

Sata, N., Shen, G., Rivers, M.L. and Sutton, S.R., 2002. Pressure-volume equation of state of high-pressure B2 phase of NaCl. Phys. Rev. B, 65: 104114.

Shen, G., Rivers, M.L., Wang, Y. and Sutton, S.R., 2001. Laser heated diamond cell system at the Advanced Photon Source for in situ x-ray measurements at high pressure and temperature. Rev. Sci. Instrum., 72: 1273-1282.

Stixrude, L. and Brown, J.M., 1998. The Earth's core. In: R.J. Hemley (Editor), Ultrahigh-pressure mineralogy. Reviews in Mineralogy. Mineralogical Society of America, Washington, D.C., pp. 261-282.

Takahashi, T. and Bassett, W.A., 1964. A high pressure polymorph of iron. Science, 145: 483-486.

Uchida, T., Wang, Y., Rivers, M.L. and Sutton, S.R., 2001. Stability field and thermal equation of state of e-iron determined by synchrotron x-ray diffraction in a multi-anvil apparatus. J. Geophys. Res., 106: 21799-21810.

Vocadlo, L. et al., 2003. Possible thermal and chemical stabilization of body-centred-cubic iron in the Earth's inner core. Nature, 424: 536-539.

Figure Captions

Figure 1. Representative XRD spectra for Fe5%Ni at 43 GPa. The sample transforms from an initially hcp phase to a mixture of hcp and fcc phases and finally to nearly entirely fcc phase with increasing temperature. Diffraction peaks from the different phases as well as those from the B2 phase of NaCl are labeled.

Figure 2. Phase relationships for Fe5%Ni, Fe15%Ni, and Fe20%Ni. The solid lines show approximate phase boundaries for the hcp + fcc two phase coexistence region. Symbols show experimental results where we observed different phases; *:hcp only; squares:hcp+ fcc; trangles:fcc only; X:melt. Lines may differ from thermodynamic equilibrium due to kinetics.

Figure 3. Schematic phase relationships for Fe-rich Fe-Ni compositions for varying *T-x* at 30, 40, 50, and 60 GPa. Circles: interpolations of our results for Fe5%Ni, Fe15%Ni, and Fe20%Ni; *: Fe (Ma et al., 2004); triangles:Fe10%Ni (Lin et al., 2002); diamonds:Fe30%Ni (Huang et al., 1992). Closed symbols and dotted lines show hcp→hcp + fcc boundary; open symbols and solid lines show hcp + fcc→fcc boundary.

Figure 4. Portion of XRD spectra for Fe20%Ni taken at 72 GPa and 1400 K at different times during a 50 minute heating cycle. At right, Bruker CCD images show that the Debye rings became much smoother with extended heating, indicating the decreasing grain size of the hcp phase equilibrating at high temperature relative to the grain size in the hcp + fcc

assemblage initially quenched from higher temperature. It took approximately 30 minutes to transform the initial mixed hcp + fcc assemblage into hcp only.

Figure 5. Conditions for the long heating cycle for Fe20%Ni at 72 GPa corresponding to Figure 4. Before this cycle, a hcp+fcc two phase mixture was synthesized at 1596 K. Dotted line indicates when power to YLF lasers was increased. Symbols show what phases were present in the *in-situ* XRD patterns taken at different times during heating. We crossed the hcp only → hcp + fcc phase boundary on both decreasing and increasing temperature to constrain this boundary within 100 K. Dashed line indicates approximate transition temperature.

Figure 6. Extrapolation of our Fe15%Ni and previously reported Fe10%Ni (Lin et al., 2002) results to core conditions. Thick solid line: Lindemann law extrapolation of hcp Fe melting curve (Ma et al., 2004); Dotted lines: hcp→hcp + fcc boundaries; thin, solid lines: hcp + fcc → fcc boundaries Shaded areas indicate two phase hcp + fcc regions. Dashed lines show the core-mantle boundary (CMB) and inner core-outer core boundary (ICB) pressures.

Table 1. $\Delta V^{fcc\text{-}hcp}$ for different compositions and *P-T* conditions

Composition	P (GPa)	T (K)	$\Delta V^{fcc\text{-}hcp}$ (%)
Fe5%Ni	43	1680	1.3
	55	2280	2.4
Fe15%Ni	39	1450	1.1
	53	1740	3.2
Fe20%Ni	62	1786	2.2
	72	1909	2.2

Table 2. Phase boundary slope for varying Ni compositions

Slope (K/GPa)	Pure Fe	Fe10%Ni	Fe15%Ni	Fe30%Ni
hcp → fcc	39.3	-	-	-
hcp → hcp + fcc	-	28.1	17.9	-
hcp + fcc → fcc	-	34.9	21.8	25

Fe10%Ni data is from (Lin et al., 2002); Fe30%Ni data from (Huang et al., 1992); Note: there was not enough data to estimate a phase boundary for Fe5%Ni and Fe20%Ni.

Figure 1

Click here to download high resolution image

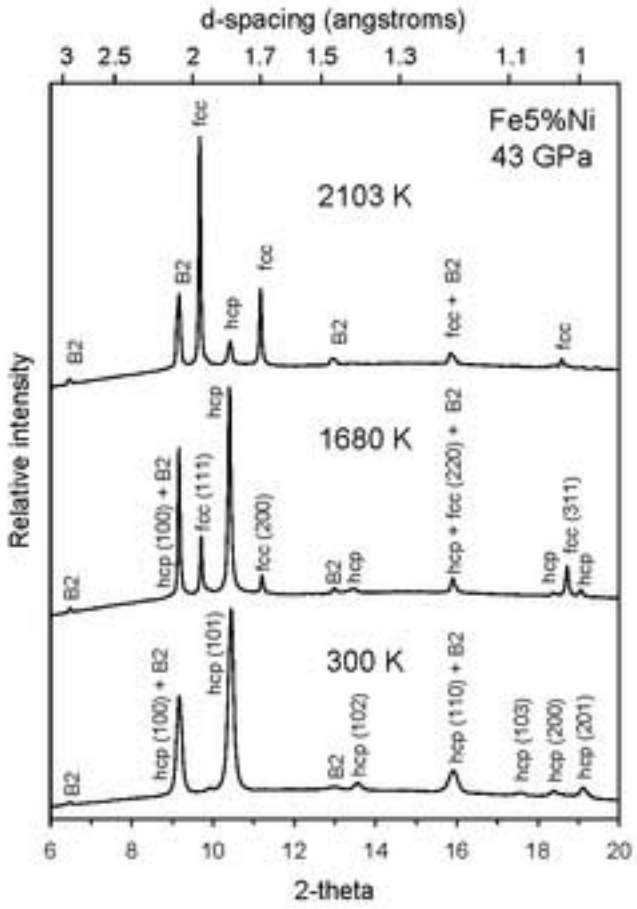

Figure 1

Figure 2

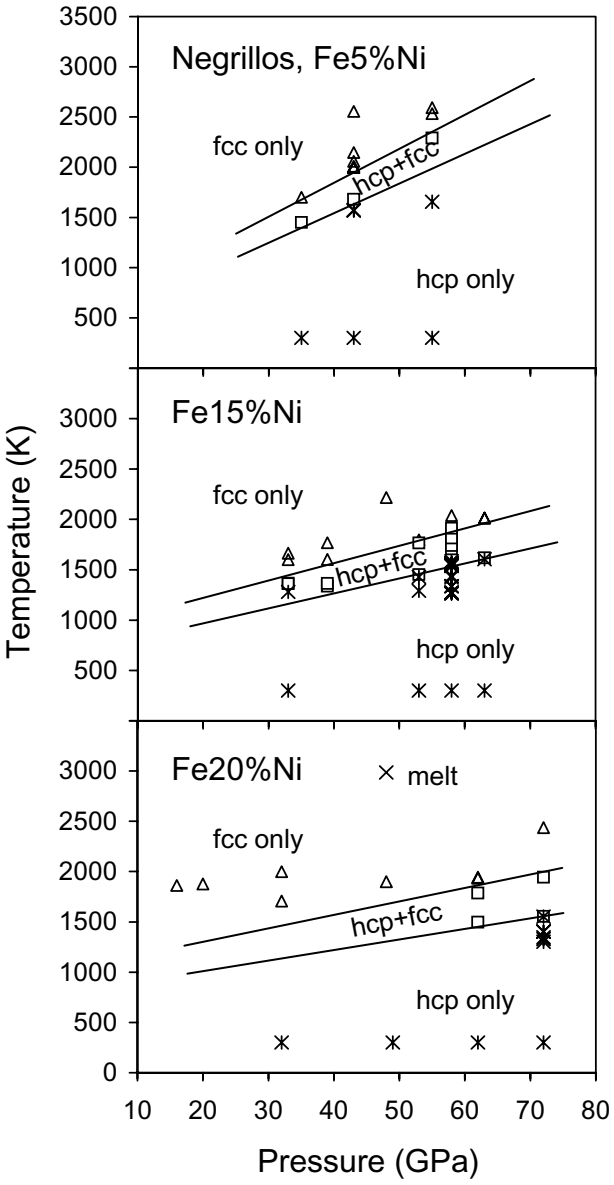

Figure 2

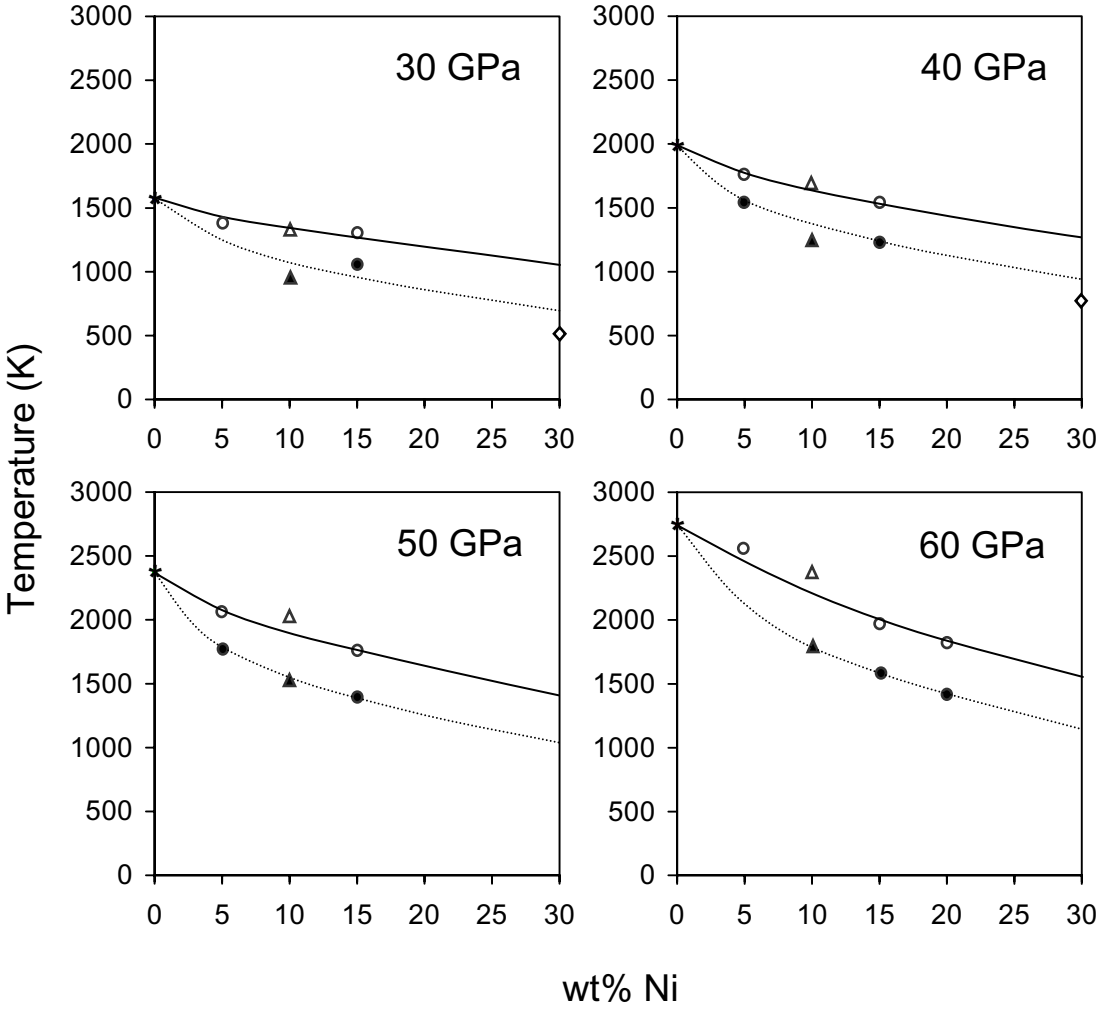
30 GPa
40 GPa
50 GPa
60 GPa
Temperature (K)
wt% Ni
0
500
1000
1500
2000
2500
3000
0
5
10
15
20
25
30

Figure 3

Figure 4

Click here to download high resolution image

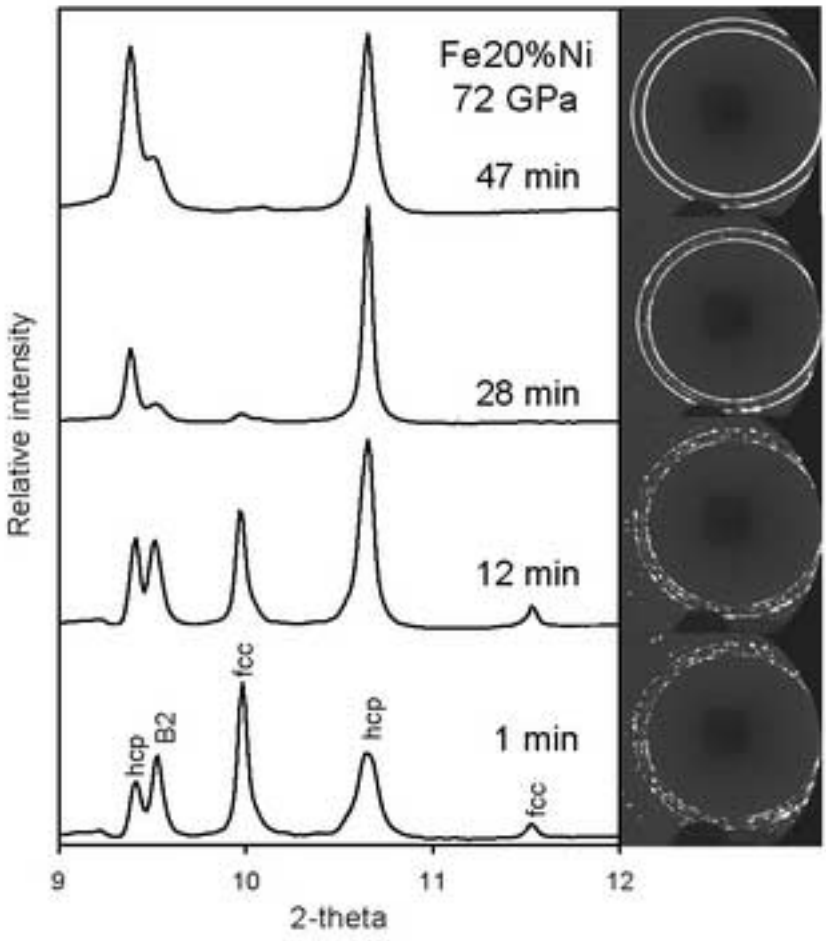

Figure 4

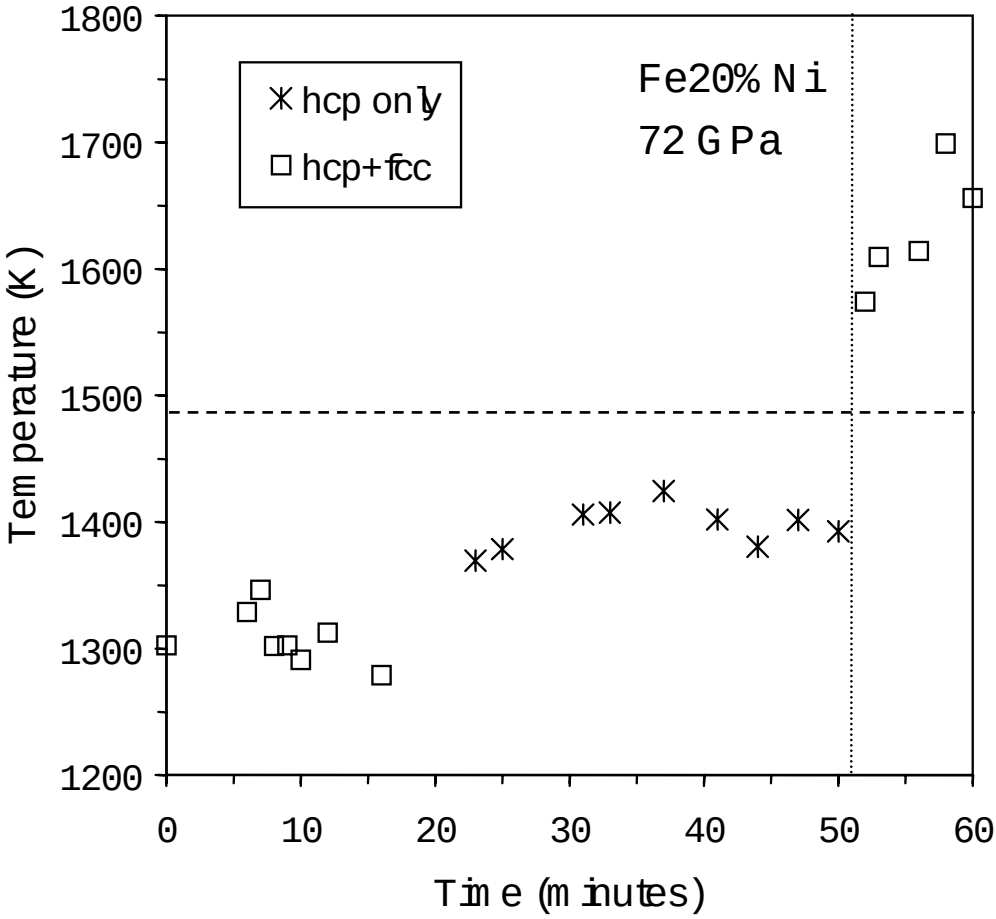
1800
1700
1600
1500
1400
1300
1200
Temperature (K)
0
10
20
30
40
50
60
Time (minutes)
hcp only
hcp+fcc
Fe20% Ni
72 GPa

Figure 5

Figure 6
Click here to download high resolution image

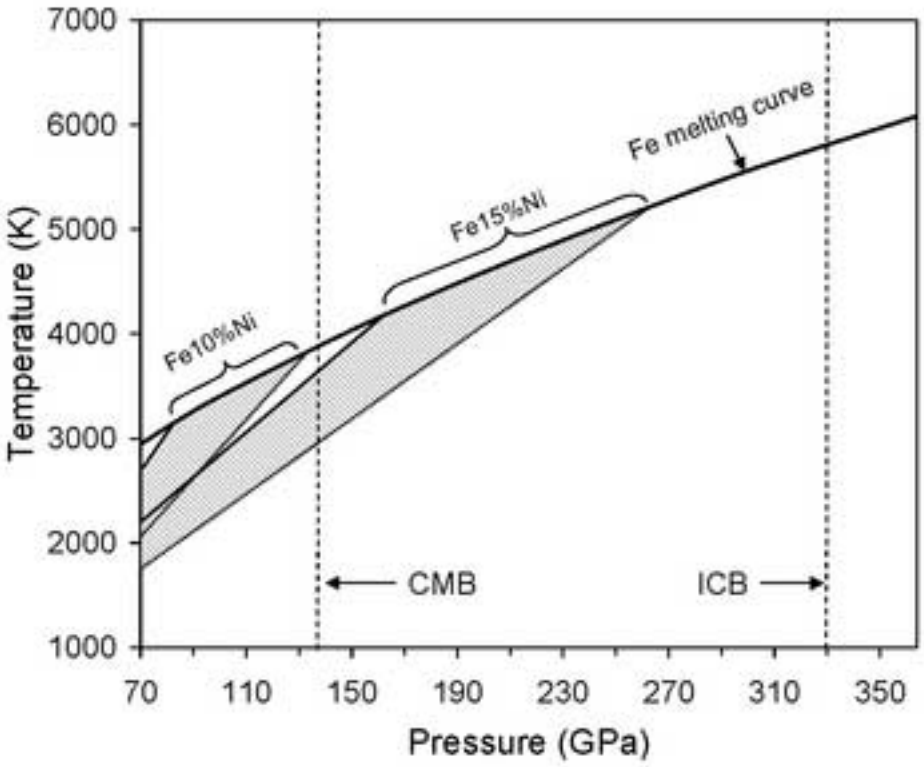

Figure 6